

70% decrease of hot-spotted photovoltaic modules output power loss using novel MPPT algorithm

Mahmoud Dhimish, *Member, IEEE*

Abstract—The phenomenon of 'Hot-spotting' within photovoltaic (PV) panels, where a mismatched cell/cells heats up, leads to reliability and efficiency issues. In this paper, a novel maximum power point tracking (MPPT) algorithm is developed to compensate for hot-spotted PV module effects, thus increasing the output power and improving reliability. The MPPT algorithm implements two mitigation processes; the first to identify the optimum power-voltage (P-V) curve to track the global maximum power point (GMPP). The second process is to manipulate the output power towards the GMPP through the control of the perturbation step size. In order to verify the appropriateness of the proposed algorithm, multiple hot-spotted PV modules were tested under various environmental conditions. Significantly, the algorithm reduces the hot-spotted PV modules output power loss by at least 70% under all irradiance transition scenarios, slow, medium, and fast.

Index Terms—Photovoltaic; Solar Energy; Hot-Spots; MPPT; GMPP; Power Mitigation; Thermal Imaging.

I. INTRODUCTION

HOT-SPOTTING is a reliability problem in Photovoltaic (PV) modules, this phenomena is well-identified when a mismatched solar cell temperature increases significantly, reducing the overall PV module output power [1]. PV hot-spots occur when a cell, or group of cells activates at reverse-bias, dissipating power instead of delivering it, and consequently operating at anomalous temperature levels [2] and [3]. The PV hot-spots are also the main cause of accelerated ageing, and sometimes irreversible damage of entire PV panels [4].

There are a number of other reliability issues affecting PV modules such as PV module disconnection [5], faults associated with maximum power point tracking (MPPT) units [6] and [7], PV micro cracks [8], and fluctuations in the wind speed and humidity variations [9]. All of these factors affect the PV module output power performance, thus decrease the annual energy production. However, this article addresses the impact of hot-spotting in PV modules and aims to reduce the PV losses.

PV Hot-spots can easily be detected through IR inspection, which has become a common practice in current PV application as presented in [10]. However, the impact of hot-spot on the

operation and performance of PV modules have been extensively investigated and addressed, which helps us to explain why there is a lack of accepted approaches which deal with hot-spotting, as well as specific criterion referring to the acceptance or rejection of affected PV module/s in commercial systems.

The typical practice of mitigating hot-spotting effects, is usually through the adoption of bypass diodes which are parallelized with the PV modules. This technique limits the maximum reverse voltage across the hot-spotted or shaded solar cells, therefore increases the overall short circuit current and the open circuit voltage [11] – [13]. However, this method of mitigating hot-spots is not considered favorable, since it requires additional costs and can even be detrimental in terms of power dissipation caused by additional bypass diodes [14].

Most recently, conventional approaches using distributive MPPT techniques to mitigate hot-spot in PV modules, suggested by S. Yang *et al.* [15] and C. Olalla *et al.* [16] show an approximate reduction up to 20 °C for small and medium hot-spotting areas. Additionally, Y. He *et al.* [17] show the perceived inadequacies of the standard bypass diodes, through the insertion of a series-connected switch which proved suited the to interrupt of the current flow during bypass activation process. However, this solution requires a relatively complex electronic circuit design, and it is relatively highly cost.

In 2018, two hot-spot mitigation techniques were developed by Dhimish *et al.* [18]. Both techniques consist of several MOSFETs connected to the PV module in order to switch ON/OFF the hot-spotted PV solar string. The proposed technique is fairly reliable, but has limited improvements on the PV modules output power.

It is of significance that under hot-spotting scenarios, the characteristics of PV modules, show multiple local maximum power points (LMPPs) and a unique global maximum power point (GMPP). Many conventional MPPT methods, such as Perturb and Observe (P&O) [19], Incremental Conductance (INC) [20], and Beta method [21] enable the GMPP to be distinguish from the LMPPs. Consequently, both the generated power and the system reliability are significantly affected. As detailed by the real data in [22], the measured power loss is from 55% to 60% due to the wrong tracking of the operating point at LMPPs.

To address the reliability issue in MPPT methods, several hardware-based systems have been industrialized, including the bypass diodes method using the integration of bypass diodes in the PV modules sub-strings [11], reconfiguration of PV modules [23], and the distributed MPPT units [15].

As an overall generic remark; there are a limited number of MPPT methods which ultimately attempt to optimize the output power of hot-spotted PV modules with respect to effectively tracking the GMPP, but not the LMPPs. In addition, there is a limited evaluation of MPPT methods on hot-spotted PV modules, since most adapted approaches were evaluated and assessed only in partial shading conditions, but not on hot-spotting scenarios. Hence, the main motivation of this work, includes (i) Development of a novel hot-spotting MPPT algorithm to enhance the output power of the affected PV modules by different types of hot-spots, and (ii) Evaluate the developed MPPT algorithm using various hot-spotting forms under standard test conditions, as well as a number of environmental states.

II. METHODOLOGY

As stated earlier, hot-spots cause reliability issues and also impact on the performance of the PV modules. Therefore, this section will analyze the impact of different hot-spots on the output power performance of PV modules.

The examined PV system shown in Fig. 1(a) comprises of 220 roof topped polycrystalline silicon PV modules. The PV modules electrical characteristics at standard test conditions (STC), where the irradiance (G) is equal to 1000 W/m^2 for a temperature (T) equal to 25°C :

- Maximum power point (P_{mpp}) : 220.2 W_p
- Voltage at maximum power point (V_{mpp}) : 28.7 V
- Current at maximum power point (I_{mpp}) : 7.67 A
- Open circuit voltage (V_{oc}) : 36.7 V
- Short circuit current (I_{sc}) : 8.18 A

Before assessing the impact of the hot-spotting phenomena on the output power performance loss of the PV modules, all other factors were excluded. The PV modules were inspected using a thermal imaging camera (FLIR i5), in order to exclude factors such as partial shading, dust, or cracks. An example of a typical thermal image is shown in Fig. 1(b).

A power-voltage (P-V) and current-voltage (I-V) curve tracer was used to measure the respective curves for the hot-spotted PV modules, and therefore compare the results to the theoretical predictions.

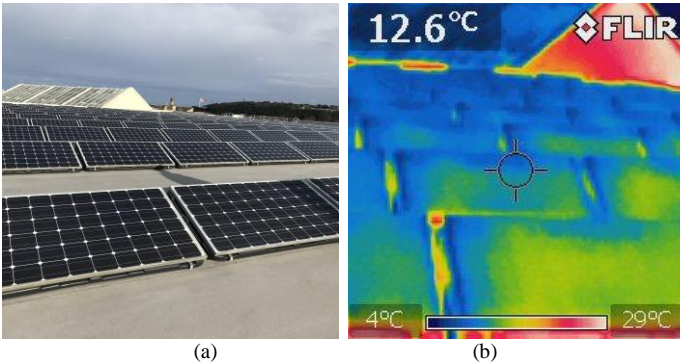


Fig. 1. Examined PV modules. (a) Real image of the inspected PV system, (b) Thermal image of several PV modules

III. PROPOSED PV HOT-SPOT MPPT ALGORITHM

The proposed PV hot-spot MPPT algorithm will be described and briefly assessed - the aim is to enhance the output power for PV modules affected by hot-spots. It is worth noting, that most MPPT techniques, either in the previously discussed literature [17] – [23] or available commercial industrialized MPPT units, are mainly to mitigate the output power of PV modules affected by partial shading conditions, whereas the impact of the hot-spots are hardly considered. Therefore, in this article the proposed technique is developed to enhance the output power of hot-spotted PV modules, and also to preserve fast and reliably MPPT approach, eventually operating at global maximum power point (GMPP) instead of the local maximum points (LMPPs). Fig. 2 shows the hot-spotted PV module GMPP and LMPP points, where it typically operates at LMPP2 through the step from LMPP1. However, a healthy PV module operates at the GMPP, where the proposed MPPT technique aims to track to this power level.

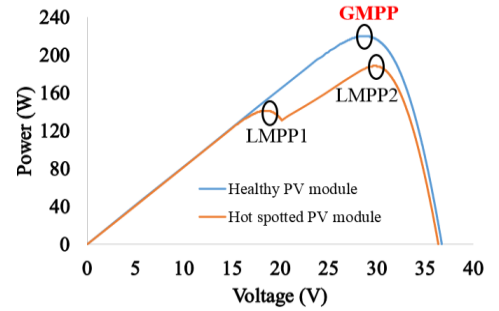


Fig.2. Global and local maximum power points

As shown in Fig. 3 the proposed MPPT technique is divided into two steps, where the first step is to identify the GMPP from the LMPPs. Identifying the GMPP allows the determination of the desirable output power level as well as the corresponding duty cycle (D_{GMPP}). To identify the GMPP it is required to store the n^{th} maximum output power for the PV module and then process all the acquired power data from zero to max-power. At this stage, the GMPP will be identified from the LMPPs. However, in order to find the duty cycle at the GMPP, initially a continuous loop is processed with the following conditions:

```

Find  $\Delta P(n) = P(n) - P(n-1)$ ;
IF  $\Delta P(n) \leq P(n) - P(n-1)$ 
{Else  $D_{\text{GMPP}} = D_{\text{GMPP}}(n-1)$ ;
Return}
 $D_{\text{GMPP}} = D_{\text{GMPP}}(n)$ ;

```

After identifying the GMPP and the duty cycle at this power level, the PV module voltage, current and power will be measured, and three thresholds, namely: 50% GMPP, 75% GMPP, and 100% GMPP selected to operate the MPPT technique at the required duty cycle.

The three thresholds were selected to step from the original P-V curve of the hot-spotted PV module to the healthy PV module curve characteristics. In most cases, 50% of the GMPP would be sufficient to start tracking the actual GMPP, but, certainly this level could be adapted based on the PV module size and internal configuration of the bypass diodes. As shown

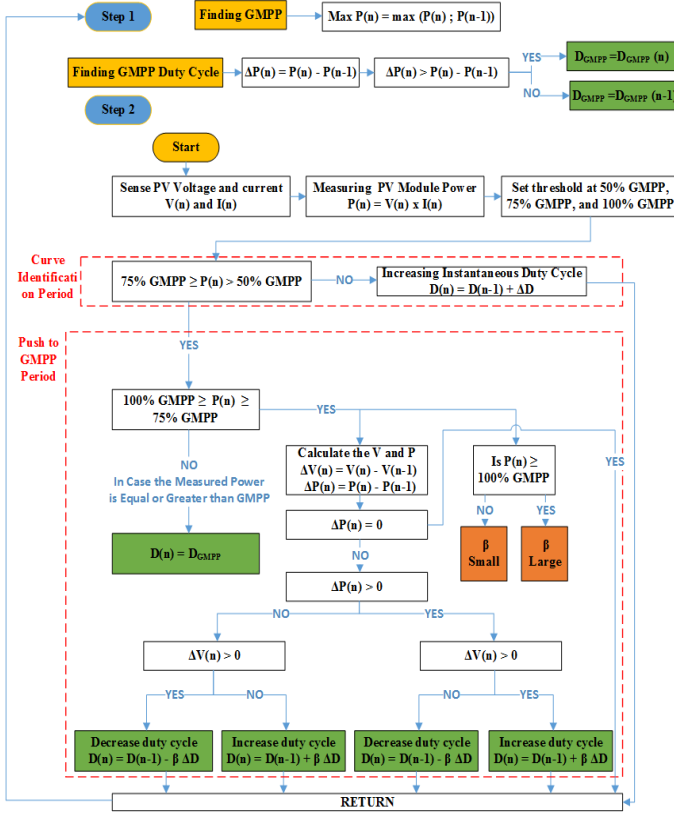


Fig. 3. Detailed description of the proposed PV hot-spotting MPPT algorithm

in Fig. 4(a), from 50% GMPP to 75% GMPP is called the curve identification period, which is the instantaneous duty cycle $D(n)$ of the MPPT algorithm equal to: $D(n) = D(n-1) + \Delta D$. Where ΔD is the fixed step size, normally starts from minimum predefined value D_{min} to its maximum value D_{max} . The D_{min} can be takes as low as 10% of the whole variation, whereas D_{max} must not exceed 90%. This operation allows the system to sweep the PV output power to identify the GMPP, as well as the corresponding GMPP duty cycle. Therefore, at 90%, $D(n)$ would remain still, unless the hot-spotted module is affected by different weather condition; or GMPP needs lower sweep at lower duty cycle.

According to Fig. 3, if the curve identification period successfully targeted 75% of the GMPP, ultimately the next step is to track the 100% GMPP threshold, starting from the 2nd threshold 75% GMPP. This period is called push to GMPP as shown in Figs. 3 and 4(a). At this stage, the difference in the voltage and power is measured, and if the difference in the output power is zero or negative, the algorithm repeats by returning back to the start point, otherwise, it will pass to the next step. The voltage difference is measured to identify whether it is positive ($\Delta V(n) > 0$) or negative ($\Delta V(n) < 0$). The differences between both regions perturbation step size ($\beta \Delta D$) will be subtracted or added to the initial duty cycle value. A large perturbation step size leads to faster GMPP convergence, subsequently operating the hot-spotted PV module near to 100% of the GMPP. It is worth noting that the value of the β is chosen according to the difference between the GMPP and the PV module output power (P) with respect to the last threshold range of 75% to 100% of the GMPP.

As the PV output power approaches the GMPP through the step size variations and the perturbation process, the perturbation step size will be reduced, thus minimizing the energy loss due to oscillations in steady-state conditions. In case the measured output power is equal to the GMPP, which ultimately is not possible to obtain, due to the hot-spot; the duty cycle at this level will be the same as the duty cycle of the GMPP at D_{GMPP} .

The proposed PV hot-spot MPPT algorithm has been implemented and experimentally mounted on the back of PV modules exhibiting hot-spots. Fig. 4(b) shows the state design of the proposed MPPT system, where initially, the PV module is inspected using a FLIR thermal camera to ensure there are hot-spots, not any other damage such as cell cracking, glass breakage, or excessive soiling. Next, the PV module is connected to a DC/DC converter, with the duty cycle controlled using the proposed MPPT algorithm.

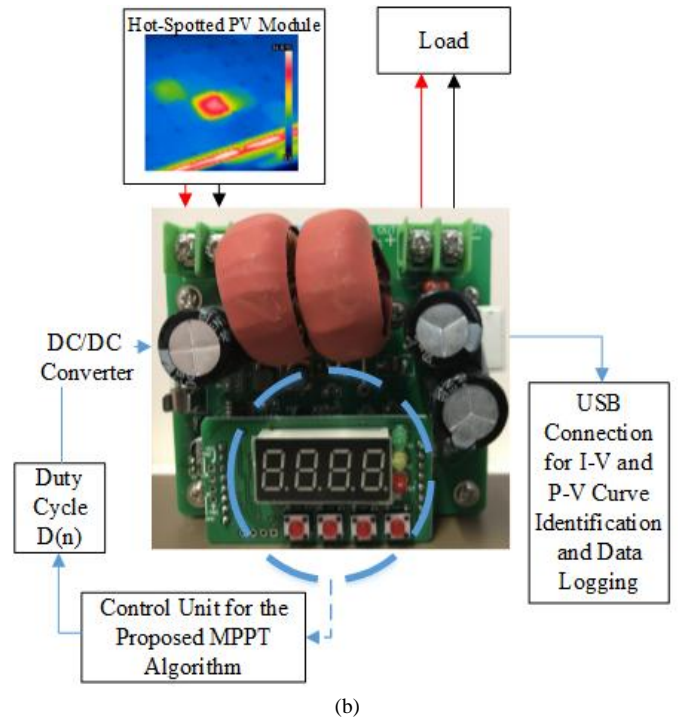
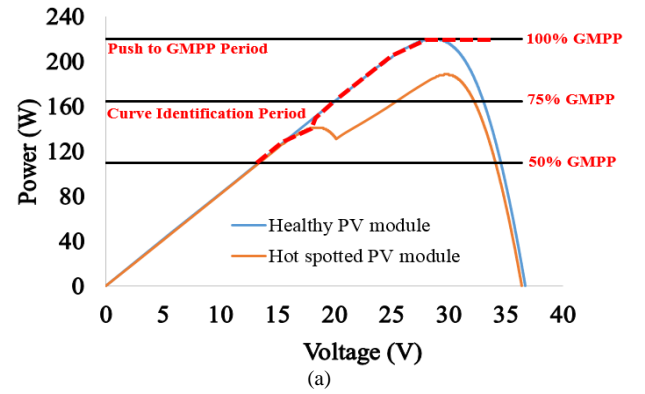


Fig. 4. (a) Curve identification period where the PV measured power is from 50% to 75% of the target GMPP, and the push to GMPP period where the PV measured power is from 75% to 100% of the target GMPP, (b) Block diagram of a hot-spotted PV module connected to the proposed technique

IV. EVALUATING THE PROPOSED MPPT TECHNIQUE

The assessment of the proposed MPPT technique will be evaluated using an analysis of the P-V curves under STC for various PV modules with different types of hot-spotted solar cells.

Fig. 5(a) shows an example of a PV module with two hot-spotted solar cells. Under STC, the PV module theoretically generate an output peak power of 220.2 W, but due to the impact of the hot-spots, the output power is measured at 208.4 W. By using the proposed MPPT unit, at 50% of the GMPP the MPPT algorithm starts to track and enhance the output P-V curve. There is a sweep in the P-V curve almost after 50% GMPP due to the fast transition (FT) of the duty cycle, because of the change in the perturbation step size ($\beta \Delta D$). Remarkably, the MPPT successfully operates at almost the GMPP and the output power increased to 217.5 W. Hence, the output power loss for the hot-spotted PV modules is reducing by 77%, this is calculated by (2).

$$\begin{aligned} \text{Reduction in PV output power loss} &= \\ 100 - \left(\frac{P_{\text{free}} - P_{\text{MPPT}}}{P_{\text{free}} - P_{\text{hot-spotted}}} \times 100 \right) &= \\ 100 - \left(\frac{220.2 - 217.5}{220.2 - 208.4} \times 100 \right) &= 77\% \end{aligned} \quad (2)$$

A PV module exhibiting three hot-spotted solar cells was tested, with the thermal image of the PV module and the P-V curve without using the proposed MPPT algorithm is shown in Fig. 5(b), where the output power is equal to 203.5 W. After using the proposed MPPT unit, and due to the high loss in the output power of the PV module, the perturbation step size ($\beta \Delta D$) of the MPPT algorithm has fast transitions (FT) at 50% GMPP (first threshold), and at 75% GMPP (second threshold). However, there is almost steady state (SS) in tracking the P-V curve of this particular PV module at almost all other voltage and power levels as shown in Fig. 5(b). After using the proposed MPPT, the PV module generates a 13.2 W power improvement to 216.7 W, compared to the system without the proposed MPPT algorithm, resulting a reduction in the PV output power loss of 79%; calculated using (2).

Additionally, the proposed MPPT algorithm is evaluated using a PV module affected by both permanent shade and two hot-spotted solar cells. An actual and thermal image of the PV module is shown in Fig. 6(a).

When under STC, the PV module generates 198.3 W, but after adopting the proposed MPPT the output power is enhanced by 18.9 W; resulting 86% of reduction in the PV output power loss.

The PV module has also been tested under two different irradiance conditions, including:

- Sunny day: slow irradiance conversion; results shown in Fig. 6(c)
- Cloudy day: fast irradiance conversion; results shown in Fig 6(d)

The reduction in the power loss of the examined PV module is 86% using the proposed MPPT technique. While as shown in Fig. 6(b), the average reduction in the output power for the hot-spotted PV module during a sunny day is equal to 82.2%.

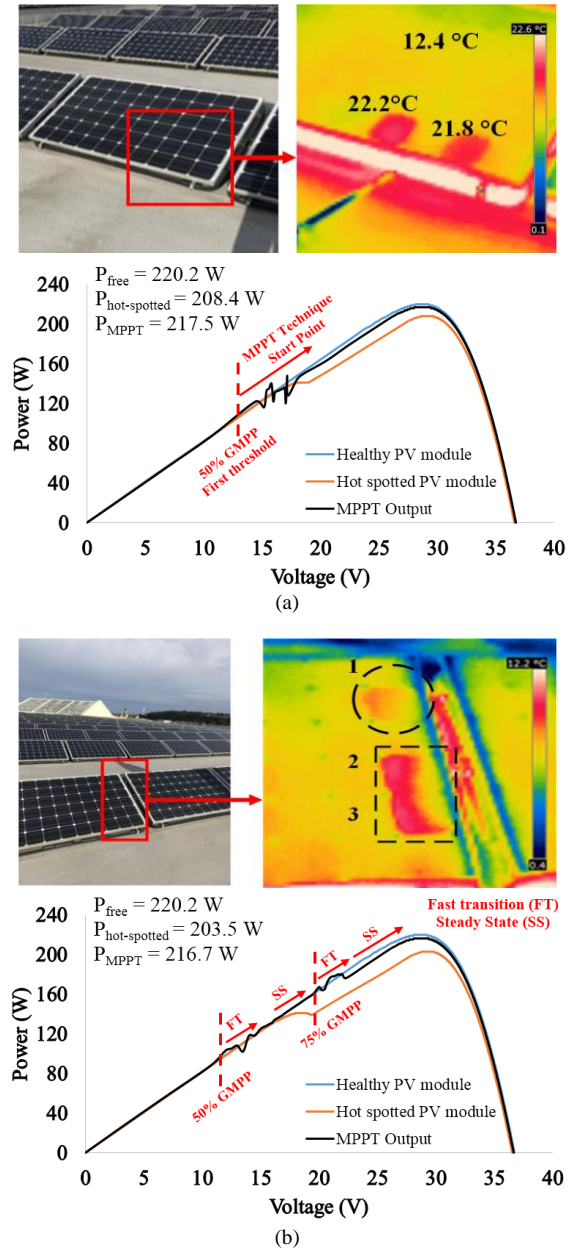
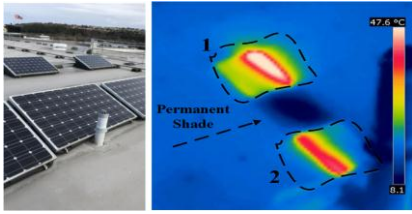


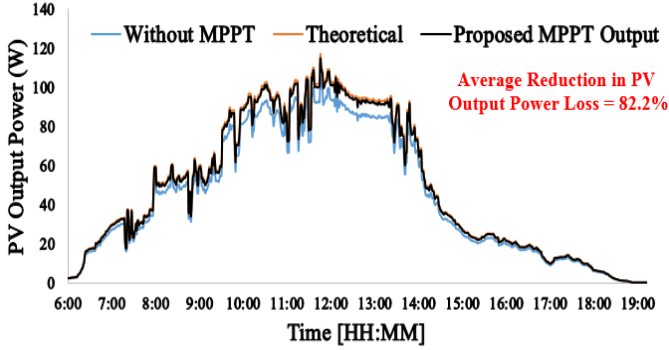
Fig. 5. Examined PV module before and after the proposed MPPT technique. (a) Thermal image of an inspected PV module affected by two hot-spotted solar cells and the difference in the P-V curves obtained for healthy, hot-spotted, and the MPPT technique, (b) Thermal image of the inspected PV module affected by three hot-spotted solar cells and the difference in the P-V curves obtained for healthy, hot-spotted, and the MPPT technique

Similar results obtained for the output measured power shown in Fig. 6(c), where the PV module is affected by fast transitions in the irradiance levels. The average reduction in the PV module output power loss is equal to 73.8%. Compared to previous results (shown in Fig. 6(a)), the drop in the reduction of the PV output power loss is due to the fast transition of the irradiance affecting the PV module, hence the identification of the GMPP is frequently updated and affected by different P-V curve characterization.

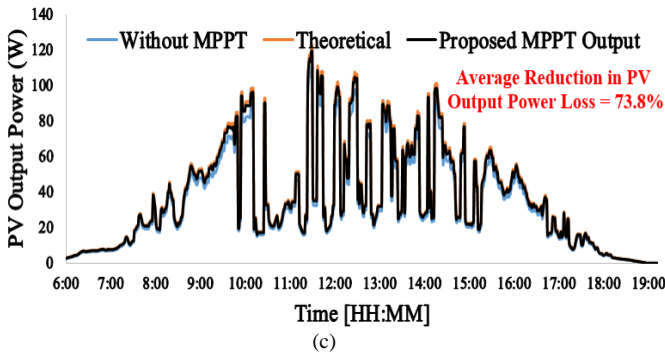
To sum up, this section presents the evaluation of the proposed MPPT technique using three different PV modules affected by diverse hot-spots. Evidently, the MPPT technique decreases the loss in the output power by at least 70%.



(a)



(b)



(c)

Fig. 6. (a) Actual and thermal image of the tested PV module, (b) Long term measured data for the tested PV module evaluated under sunny day – slow irradiance transition, (c) Long term measured data for the tested PV module under cloudy day – fast irradiance transition

V. CONCLUSION

It has been determined that only a limited number of MPPT techniques adopted to enhance hot-spotted PV modules output power, and the characteristics of hot-spotted PV modules are different to those established by partial shading scenarios. Therefore, in this paper we present the development of novel MPPT algorithm to enhance hot-spotted PV modules output power.

The developed MPPT algorithm utilizes two processes; first is the curve identification period, which lies within two threshold values, namely 50% GMPP and 75% GMPP. If the curve identification period successfully targeted 75% of the GMPP, ultimately next step is to track the 100% GMPP threshold, starting from the second threshold 75% GMPP; This period/process is called push to GMPP.

In order to verify the appropriateness of the proposed algorithm, the algorithm has been implemented and experimentally mounted on the back of PV modules exhibiting multiple hot-spots. The PV modules are affected by either two or three hot-spotted solar cells, or permanent shade patterns. Significantly, the algorithm reduces the loss in output power in the range of 77% to 83% for slow irradiance transitions. While, at medium and fast irradiance transitions, the algorithm reduces the output power loss in the range of 70% to 75%.

REFERENCES

- [1] S. Raimondi Cominesi, M. Farina, L. Giulioni, B. Picasso and R. Scattolini, "A Two-Layer Stochastic Model Predictive Control Scheme for Microgrids," in *IEEE Transactions on Control Systems Technology*, vol. 26, no. 1, pp. 1-13, Jan. 2018, doi: 10.1109/TCST.2017.2657606.
- [2] M. Dhimish, V. Holmes, P. Mather, and M. Sibley, "Novel hot spot mitigation technique to enhance photovoltaic solar panels output power performance," in *Solar Energy Materials and Solar Cells*, vol. 179, pp. 72-79, June 2018, doi: 10.1016/j.solmat.2018.02.019.
- [3] C. Peng, M. Wu and D. Yue, "Working Region and Stability Analysis of PV Cells Under the Peak-Current-Mode Control," in *IEEE Transactions on Control Systems Technology*, vol. 26, no. 1, pp. 352-359, Jan. 2018, doi: 10.1109/TCST.2017.2661827.
- [4] R. D. Prabha and G. A. Rincón-Mora, "Drawing the Most Power From Low-Cost Single-Well 1-mm2CMOS Photovoltaic Cells," in *IEEE Transactions on Circuits and Systems II: Express Briefs*, vol. 64, no. 1, pp. 46-50, Jan. 2017, doi: 10.1109/TCSII.2016.2546907.
- [5] X. Guo, "A Novel CH5 Inverter for Single-Phase Transformerless Photovoltaic System Applications," in *IEEE Transactions on Circuits and Systems II: Express Briefs*, vol. 64, no. 10, pp. 1197-1201, Oct. 2017, doi: 10.1109/TCSII.2017.2672779.
- [6] H. Li, D. Yang, W. Su, J. Lü and X. Yu, "An Overall Distribution Particle Swarm Optimization MPPT Algorithm for Photovoltaic System Under Partial Shading," in *IEEE Transactions on Industrial Electronics*, vol. 66, no. 1, pp. 265-275, Jan. 2019, doi: 10.1109/TIE.2018.2829668.
- [7] T. Qian, "A Converter Combination Scheme for Efficiency Improvement of PV Systems," in *IEEE Transactions on Circuits and Systems II: Express Briefs*, vol. 65, no. 11, pp. 1668-1672, Nov. 2018, doi: 10.1109/TCSII.2017.2764027.
- [8] M. Dhimish, V. Holmes, B. Mehrdadi, and M. Dales, "The impact of cracks on photovoltaic power performance," in *Journal of Science: Advanced Materials and Devices*, vol. 2, no. 2, pp. 199-209, 2017, doi: 10.1016/j.jsamd.2017.05.005.
- [9] N. G. Dhere, N. S. Shiradkar and E. Schneller, "Evolution of Leakage Current Paths in MC-Si PV Modules From Leading Manufacturers Undergoing High-Voltage Bias Testing," in *IEEE Journal of Photovoltaics*, vol. 4, no. 2, pp. 654-658, March 2014, doi: 10.1109/JPHOTOV.2013.2294764.
- [10] M. Dhimish, P. Mather and V. Holmes, "Evaluating Power Loss and Performance Ratio of Hot-Spotted Photovoltaic Modules," in *IEEE Transactions on Electron Devices*, vol. 65, no. 12, pp. 5419-5427, Dec. 2018, doi: 10.1109/ED.2018.2877806.
- [11] M. Lasheen, A. K. Abdel Rahman, M. Abdel-Salam and S. Ookawara, "Adaptive reference voltage-based MPPT technique for PV applications," in *IET Renewable Power Generation*, vol. 11, no. 5, pp. 715-722, 12 4 2017, doi: 10.1049/iet-rpg.2016.0749.
- [12] F. Wang, T. Zhu, F. Zhuo and H. Yi, "An Improved Submodule Differential Power Processing-Based PV System With Flexible Multi-MPPT Control," in *IEEE Journal of Emerging and Selected Topics in Power Electronics*, vol. 6, no. 1, pp. 94-102, March 2018, doi: 10.1109/JESTPE.2017.2719919.
- [13] M. Dhimish, V. Holmes, B. Mehrdadi, M. Dales, and P. Mather, "PV output power enhancement using two mitigation techniques for hot spots and partially shaded solar cells," in *Electric Power Systems Research*, vol. 158, pp. 15-25, 2018, doi: 10.1016/j.epsr.2018.01.002.
- [14] A. A. Abdelmoaty, M. Al-Shyouchk, Y. Hsu and A. A. Fayed, "A MPPT Circuit With 25 μW Power Consumption and 99.7% Tracking Efficiency for PV Systems," in *IEEE Transactions on Circuits and Systems I: Regular Papers*, vol. 64, no. 2, pp. 272-282, Feb. 2017, doi: 10.1109/TCSI.2016.2604224.
- [15] S. Yang, K. Itako, T. Kudoh, K. Koh and Q. Ge, "Monitoring and Suppression of the Typical Hot-Spot Phenomenon Resulting From Low-Resistance Defects in a PV String," in *IEEE Journal of Photovoltaics*, vol. 8, no. 6, pp. 1809-1817, Nov. 2018, doi: 10.1109/JPHOTOV.2018.2861734.
- [16] C. Olalla, Md. Hasan, C. Deline, and D. Maksimovic, "Mitigation of Hot-Spots in Photovoltaic Systems Using Distributed Power Electronics," in *Energies*, vol. 11, no. 4, pp. 726, 2018, doi: 10.3390/en11040726.
- [17] Y. He, B. Du and S. Huang, "Noncontact Electromagnetic Induction Excited Infrared Thermography for Photovoltaic Cells and Modules Inspection," in *IEEE Transactions on Industrial Informatics*, vol. 14, no. 12, pp. 5585-5593, Dec. 2018, doi: 10.1109/TII.2018.2822272.
- [18] M. Dhimish, V. Holmes, B. Mehrdadi, M. Dales, and P. Mather, "Output-Power Enhancement for Hot Spotted Polycrystalline Photovoltaic Solar Cells," in *IEEE Transactions on Device and Materials Reliability*, vol. 18, no. 1, pp. 37-45, March 2018, doi: 10.1109/TDMR.2017.2780224.
- [19] S. Mohanty, B. Subudhi and P. K. Ray, "A Grey Wolf-Assisted Perturb & Observe MPPT Algorithm for a PV System," in *IEEE Transactions on Energy Conversion*, vol. 32, no. 1, pp. 340-347, March 2017, doi: 10.1109/TEC.2016.2633722.
- [20] P. Zhang, G. Zhang and H. Du, "Circulating Current Suppression of Parallel Photovoltaic Grid-Connected Converters," in *IEEE Transactions on Circuits and Systems II: Express Briefs*, vol. 65, no. 9, pp. 1214-1218, Sept. 2018, doi: 10.1109/TCSII.2017.2789215.
- [21] S. Tang, Y. Sun, Y. Chen, Y. Zhao, Y. Yang and W. Szeo, "An Enhanced MPPT Method Combining Fractional-Order and Fuzzy Logic Control," in *IEEE Journal of Photovoltaics*, vol. 7, no. 2, pp. 640-650, March 2017, doi: 10.1109/JPHOTOV.2017.2649600.
- [22] H. Li, D. Yang, W. Su, J. Lü and X. Yu, "An Overall Distribution Particle Swarm Optimization MPPT Algorithm for Photovoltaic System Under Partial Shading," in *IEEE Transactions on Industrial Electronics*, vol. 66, no. 1, pp. 265-275, Jan. 2019, doi: 10.1109/TIE.2018.2829668.
- [23] T. Cheng, D. D. Lu and L. Qin, "Non-Isolated Single-Inductor DC/DC Converter With Fully Reconfigurable Structure for Renewable Energy Applications," in *IEEE Transactions on Circuits and Systems II: Express Briefs*, vol. 65, no. 3, pp. 351-355, March 2018, doi: 10.1109/TCSII.2017.2712286.